

DEK1 displays a strong subcellular polarity during *Physcomitrella patens* 3D growth

Pierre-François Perroud¹ , Rabea Meyberg¹ , Viktor Demko² , Ralph S. Quatrano³ , Odd-Arne Olsen⁴ 
and Stefan A. Rensing^{1,5,6} 

¹Plant Cell Biology, Faculty of Biology, University of Marburg, Karl-von-Frisch Str. 8, Marburg 35043, Germany; ²Department of Plant Physiology, Faculty of Natural Sciences, Comenius University in Bratislava, Ilkovicova 6, Bratislava 84215, Slovakia; ³Department of Biology, Washington University in St Louis, One Brookings Dr., Campus, Box 1137, St Louis, MO 63130, USA; ⁴Norwegian University of Life Sciences, PO Box 5003, Aas NO-1432, Norway; ⁵BIOSS Centre for Biological Signalling Studies, University of Freiburg, Schänzlestraße 18, Freiburg im Breisgau 79104, Germany; ⁶LOEWE Center for Synthetic Microbiology (SYNMIKRO), University of Marburg, Hans-Meerwein-Straße 6, Marburg 35043, Germany

Summary

Authors for correspondence:

Pierre-François Perroud
Tel: +49 6421 282 2040
Email: perroud@staff.uni-marburg.de

Odd-Arne Olsen
Tel: +37 9158 1293
Email: odd-arne.olsen@nmbu.no

Received: 26 November 2019
Accepted: 24 December 2019

New Phytologist (2020) 226: 1029–1041
doi: 10.1111/nph.16417

Key words: 3D development, cell polarity, DEK1, *Physcomitrella patens*, spermatozoid, subcellular localization.

- Defective Kernel 1 (DEK1) is genetically at the nexus of the 3D morphogenesis of land plants. We aimed to localize DEK1 in the moss *Physcomitrella patens* to decipher its function during this process.
- To detect DEK1 *in vivo*, we inserted the *tdTomato* fluorophore into *PpDEK1* gene locus. Confocal microscopy coupled with the use of time-gating allowed the precise DEK1 subcellular localization during 3D morphogenesis.
- DEK1 localization displays a strong polarized signal, as it is restricted to the plasma membrane domain between recently divided cells during the early steps of 3D growth development as well as during the subsequent vegetative growth. The signal furthermore displays a clear developmental pattern because it is only detectable in recently divided and elongating cells. Additionally, DEK1 localization appears to be independent of its calpain domain proteolytic activity.
- The DEK1 polar subcellular distribution in 3D tissue developing cells defines a functional cellular framework to explain its role in this developmental phase. Also, the observation of DEK1 during spermatogenesis suggests another biological function for this protein in plants. Finally the DEK1-tagged strain generated here provides a biological platform upon which further investigations into 3D developmental processes can be performed.

Introduction

Terrestrialization resulted in profound biochemical, developmental and morphological changes in the green lineage in response to the new environmental conditions such as reduced water availability, increased UV radiation exposure or the increase of gravity effect due the loss of water buoyancy (Rensing, 2018). A major morphological innovation was the complex meristem that generates plant 3D organs we observe today such as stem, leaf or root (Harrison, 2017). The growth coordination of such tissue requires a positional information system to control growth boundary, and the protein DEK1 (Defective Kernel 1) is identified among several others (Moody, 2019) as a key component of this process in land plants. From bryophyte to angiosperm, DEK1 is necessary for precise and coordinated cell wall positioning during the early cell division of 3D tissue establishment (Olsen *et al.*, 2015). In maize (*Zea mays*) (Becraft *et al.*, 2002; Lid *et al.*, 2002), rice (*Oryza sativa*) (Hibara *et al.*, 2009) as well as in *Arabidopsis* (*Arabidopsis thaliana*) (Johnson *et al.*, 2005; Lid *et al.*, 2005), the *dek1* null mutation leads to failure of the

embryo to establish a proper protoderm cell. Likewise in *Physcomitrella* (*P. patens*), the *PpDek1* deletion stops bud development before the establishment of any complex 3D structure (Perroud *et al.*, 2014). Analyses of non-null *dek1* mutants have confirmed the importance of DEK1 in plant body development and tissue integrity through cell wall misplacement (Tian *et al.*, 2007; Johnson *et al.*, 2005; Lid *et al.*, 2005) and cell wall composition modification (Amanda *et al.*, 2016). Partial *PpDek1* deletions result in morphological defects in every gametophytic tissues (Demko *et al.*, 2014; Johansen *et al.*, 2016). In addition to gametophytic and sporophytic 3D tissue development, DEK1 is necessary for endosperm development in angiosperms. The single aleurone cell layer, the pseudo-epidermis bordering the starchy endosperm, is missing in the maize *dek1* null mutant (Lid *et al.*, 2002). This observation was confirmed with the loss of aleurone cell fate identity in the maize mini-endosperm system in the absence of *dek1* (Gruis *et al.*, 2006). These observations led to the establishment of the model in which DEK1 acts as a plant surface sensor that detects outer tissue boundaries. DEK1 both affects cellular events leading to specific cell plate deposition and

triggers the gene expression patterns necessary for epidermis initiation and maintenance (Gruis *et al.*, 2006; Olsen *et al.*, 2015).

DEK1 is a large multi-domain protein 240 kDa in length. Its primary amino acid sequence shows a conserved modular structure across land plants (Lid *et al.*, 2002; Tian *et al.*, 2007). DEK1 presents two major topological segments, both of which are important for DEK1 function. The membrane segment or MEM domain contains 23 predicted trans membrane (TM) domains interrupted by a c. 300 amino acid residue Loop domain (Demko *et al.*, 2014). MEM mutant analyses in *Arabidopsis* (Tian *et al.*, 2007; Lid *et al.*, 2005), rice (Hibara *et al.*, 2009) and *Physcomitrella* (Demko *et al.*, 2014) indicate that this domain is necessary for proper DEK1 function. Structurally, the TM domains located after the Loop domain display similarity with the Major Facilitator Superfamily of Membrane Transporters (MFS), suggesting the potential presence of a pore within this domain (Demko *et al.*, 2014). Recently, DEK1 has been associated with a newly observed mechanosensing response, the Rapid Mechanosensing Activity (RMA) in *Arabidopsis* (Tran *et al.*, 2017), hinting at the potential nature of the signal perceived and transduced by DEK1. The RMA, defined as a rapid Ca²⁺ mechanosensing response, is independent of the well-characterized MscS-like (MSL) dependent plant mechanosensing answer (see review by Hamilton *et al.*, 2015) and depends on the presence either of DEK1 or the DEK1-MEM domain in the tested cells. There is no direct experimental evidence that DEK1 has an intrinsic Ca²⁺ channel activity, although it remains possible. However, DEK1 may interact with other Ca²⁺ transporters such as Piezo-type (Tran *et al.*, 2017; Guerringue *et al.*, 2018) and thus affect RMA Ca²⁺ intake. In any case the signal perceived by DEK1 appears to be related to differential membrane tension at the surface of the cell (Malivert *et al.*, 2018). The DEK1 cytosolic domain contains the well-conserved calpain domain. The DEK1 calpain domain consists of CysPc, the signature catalytic domain of calpains in all eukaryotic kingdoms (Zhao *et al.*, 2012), and the regulatory C2L, a C2-like domain, which also is shared with classical animal calpains (Ono & Sorimachi, 2012). Calpains are generally defined as Ca²⁺-dependent specific cysteine proteases (Ono & Sorimachi, 2012). DEK1-Calpain domain is identified as the main signal transducer of DEK1 function as its overexpression alone can rescue *dek1* null mutants both in angiosperms (Johnson *et al.*, 2008; Liang *et al.*, 2013) and in bryophytes (Perroud *et al.*, 2014). The calpain proteolytic activity requires the presence of a so-called conserved catalytic amino acid triad initially identified in mammalian calpain (Arthur *et al.*, 1995; Hosfield *et al.*, 1999) and present in plant calpain. In maize *ZmCalpain* cysteine 71, part of the triad, is indeed necessary for *in vitro* proteolytic activity (Wang *et al.*, 2003). *In vivo*, the mutation of the same amino acid abolishes the DEK1 function in *Arabidopsis* (Johnson *et al.*, 2008) and in *Physcomitrella* (Johansen *et al.*, 2016).

Critical to any further elucidation of the role of DEK1 is where it is localized. DEK1 has been detected at the plasma membrane (PM) and associated with small cytoplasmic vesicles, potential endosomes, of maize cells (Tian *et al.*, 2007). This PM localization furthermore was confirmed in *Arabidopsis* with ectopic expression *AtDek1* cDNAs fused in C-terminal to green fluorescent protein (GFP) in the *dek1-3* mutant and in WT. It showed an enriched signal in the

PM as well as a signal-associated endomembrane compartment as endoplasmic reticulum (ER) in roots and flower tissues (Johnson *et al.*, 2008; Qu *et al.*, 2014). However, ectopic expression of *AtCalpain* cDNAs fused in C-terminal to GFP in the *dek1-3* mutant was detected in the cytoplasm and in the ER around the nucleus. In both cases, no nuclear signal was detected (Johnson *et al.*, 2008). Finally, *in situ* immunolocalization using an antibody raised against *Physcomitrella* DEK1 localized *PpDEK1* at the periphery of phyllid cells was consistent with a PM localization (Perroud *et al.*, 2014).

Here we present the *in vivo* localization of DEK1 through tagging the *P. patens* gene with a fluorescent protein in its native genomic locus. The observed signal displays a clear polar subcellular distribution during 3D tissue growth. This signal is linked to the early stages of cell division and elongation, because cells of fully developed 3D tissue no longer display the fluorescent signal. Finally we show that DEK1 polar distribution is not dependent on the proteolytic activity of its calpain domain. One cell type displays a different signal: during spermatogenesis, the developing spermatozoid cell displayed a strong peripheral signal as the released spermatozoid lost rapidly any detectable signal.

Materials and methods

Plant materials and culture procedures

The *Physcomitrella patens* ecotype Grandsden used previously (Perroud *et al.*, 2014) was used as control and for transformation in the present study. A standard incubator temperature was set to 22°C with a photoperiod of 16 h : 8 h, light (70 μmol s⁻¹ m⁻²) : dark. Routine tissue culture was performed by forceps inoculation of gametophytic tissue on agarized (0.7%) BCD medium supplemented with 5 mM ammonium tartrate dibasic (BCDA) medium (Cove *et al.*, 2009). To obtain homogenous protonema culture, gametophytic tissue was blended weekly in sterile water using an homogenizer and plated onto BCDA tissue overlaid with cellophane. Tissue used either for protoplast generation or inoculum spotting was homogenized twice before use to obtain an entrained and homogenous protonemal culture. All phenotypic analyses were performed with tissue grown on BCD medium (Cove *et al.*, 2009). Likewise, the tissue samples used for RNA extraction were grown from single manual spot inocula for 14 d on BCD medium. For bud counting, cultures were initiated by pipetting 5 μl fresh blendate as described above into a regular array of 4 × 4 spots per 9 cm Petri dish. Such cultures were incubated for 2 wk in standard growth conditions and bud number was evaluated. Protoplast generation was performed as described previously (Cove *et al.*, 2009). Gametogenesis and sporophyte culture were performed as described previously (Perroud *et al.*, 2019). Antheridium and spermatozoid isolation were performed as described previously (Meyberg *et al.*, 2019) between 21 to 30 d after juvenile gametophore transfer to 15°C, with a photoperiod of 8 h : 16 h, light (20 μmol s⁻¹ m⁻²) : dark.

Molecular procedures

Sequence information was obtained from publicly available databases and nucleotide numberings are relative to the ATG start

site in the *Physcomitrella* DEK1 gene sequence (Pp3c17_17550V3.1; Lang *et al.*, 2018) unless otherwise stated. The DNA oligonucleotides (Merck, Darmstadt, Germany) used in this study are listed in the Supporting Information Table S1. If not mentioned otherwise, restriction enzymes and taq polymerases (OneTaq for routine amplification, Q5 for reverse transcription (RT)-PCR) were obtained from NEB (Ipswich, MA, USA) and used according to the manufacturer's specifications. Moss genomic DNA extraction for PCR diagnosis was as performed previously (Cove *et al.*, 2009). The genomic DNA used for Southern blot procedures was extracted with the Nucleon PhytoPure kit (GE Healthcare Life Sciences, Marlborough, MA, USA) following the manufacturer's instructions. Moss total RNA extraction was performed with 14-d-old plants grown on BCD medium using the RNeasy Plant Mini Kit (Qiagen) following the manufacturer's protocol. cDNA synthesis was performed the SuperScript™ III Reverse Transcriptase (Thermo-Fisher Scientific, Waltham, MA, USA) following the manufacturer's instructions.

Vector design and sequence assembly

The fluorescent protein gene insertion vector (pDEK1-tomato-insertion) comprises three segments: a 5' sequence composed of *PpDEK1* genomic sequence in which the tomato fluorescent protein coding sequence has been inserted in the exon 23; a hygromycin resistance cassette flanked with *LoxP* recognition sequence; and a 3' sequence composed of *PpDEK1* genomic sequence (see Fig. 1a, yellow box, for schematic representation).

The 5' segment is formed of the nucleotide 10553–11561 of *PpDEK1* genomic sequence plus, inserted at the position 11562, the ORF of *tdTomato* without the stop codon (Shaner *et al.*, 2004) and the end of the exon 23 with a short section of the following intron (nucleotides 11563–11638). Additionally, this segment was flanked by the restriction enzymes *AvrII* and *XhoI*. The 3' sequence was composed of nucleotides 11639–12646 of the *PpDEK1* genomic sequence flanked by the restriction enzymes *SpeI* and *MluI*. Each segment was cloned sequentially unto pBHRH (Schaefer *et al.*, 2010) using the restriction enzymes flanking the 3' and 5' sequences to produce the transformation vector pDEK1-tomato-insertion. The fragment syntheses and cloning were ordered and performed by GenScript (Piscataway, NJ, USA). Before transformation, the vector was linearized using the restriction enzymes *AvrII* and *MluI*.

The vector pArrow-DEK1° described previously in Johansen *et al.* (2016) was used to generate the calpain null mutation. Prior transformation, pArrow-DEK1° was cut with the restriction enzymes *SmaI* and *PacI*.

Moss transformation

Protoplast polyethylene glycol (PEG)-mediated transformation was performed by the standard procedure described previously (Cove *et al.*, 2009) using either open linear DNA for stable transformation or circular plasmid for transient transformation. Cre recombinase transient expression was as performed previously (Perroud & Quatrano, 2006; Trouiller *et al.*, 2006).

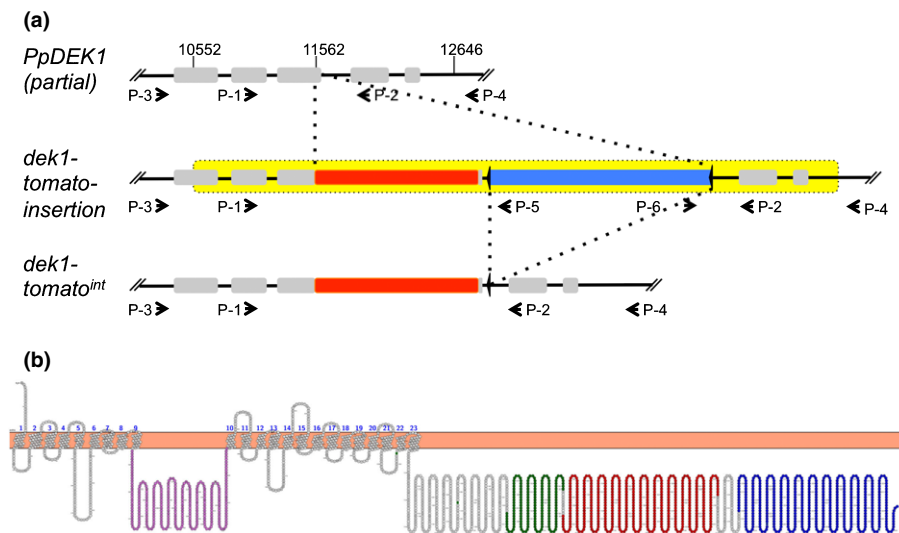


Fig. 1 Schematic representations of the *dTomato* insertion locus in the *Physcomitrella patens* genome before and after transformations (a) and of the tagged Defective Kernel 1 protein DEK1-TOMATO^{INT} (b). (a) Illustration of the wild-type (WT) and transformed loci leading to the establishment of *dekl1-tomato*^{int}. Black bar, genomic sequence; grey boxes, exon sequences; red box, *tdTomato* sequence; blue box, 35S:HPTII-CamVter resistance cassette sequence; black arrowhead, pLox sites; yellow box, transformation vector pArrowf1 insertion sequence. The dotted lines point to the vector insertion between the WT locus and the primary transformant *dekl1-pArrowf1* as well as the elimination of the resistance cassette between the primary transformant *dekl1-pArrowf1-1* and the final transformant *dekl1-tomato*^{int} upon Cre recombinase treatment. Arrows represents the primer position and orientation used in the genotyping procedure. The bp values above the WT schematic indicate (respectively) the beginning of the insertion vector, the *tdTomato* insertion site and the end of the transformation vector. (b) Schematic representation of the DEK1-TOMATO^{INT} protein using Protter (Omasits *et al.*, 2014). Orange bar, plasma membrane; amino acid labelled in fuchsia, LOOP domain; Amino acid labelled in green, LG3 domain; Amino acid labelled in red, TOMATO domain; Amino acid labelled in blue, Calpain domain.

Southern blot analysis

Southern blot was performed as described previously (Perroud & Quatrano, 2006) using 1 µg of genomic DNA per digestion. Probes were synthesized with a PCR kit (Roche) according to the manufacturer's instructions. The locus-specific 5' targeting fragment was used as a template for the primer pair P6-P7 to make the 5' probe. A locus-specific 3' targeting fragment was used as a template for the primer pair P8-P9 to make the 3' probe. The hygromycin probe was obtained by amplifying a hygromycin coding fragment using the primer pair P10-P11 with empty pBHRH vector as template. Finally, the *tdTomato* probe was produced by amplifying a *tdTomato* partial fragment using the primer pair P12-P13 using the *tdTomato* cDNA as template. Probe hybridizations were performed successively with the same membrane after stripping the previous probe as follows. The membrane first was rinsed for 5 min in deionized water. Then, the membrane was incubated in 0.5 M NaOH + 0.5 SDS at 37°C for 15 min twice. Finally, the membrane was neutralized in 1 × SCC for 20 min before starting the next hybridization cycle.

Spermatozoid staining

Spermatozoids were isolated from a mature antheridium as described previously (Meyberg *et al.*, 2019). They were dried rapidly, fixed on a glass slide and subsequently stained with DAPI before being mounted for microscopy observation.

Standard microscopy procedure

Routine tissue check and early phenotype analyses were performed with an S8 APO binocular (Leica, Wetzlar, Germany). Microscopic pictures were taken with an upright DM6000 equipped with a DFC295 camera (Leica). The LEICA APPLICATION SUITE v.4.4 was used as acquisition tool. Subsequent image processing (brightness and contrast adjustment) was performed with Adobe PHOTOSHOP Suite.

Confocal microscopy procedure

All confocal microscopy acquisitions were performed using a Leica TCS SP8X fitted with a pulsed white-light laser (commercially, WLL) and both standard photomultiplier (PMT) detector and HyD™ detector. Observation and image acquisition were done using the Leica Application Suite X (LAS X) according to the manufacturer's instructions. For live imaging of dTomato tagged protein, the excitation wavelength was set to 554 nm, and the optimal excitation wavelength of the *tdTomato* fluorophore and the signal acquisition was performed between 578–590 nm using the HyD™ detector. Additionally the signal was gated between 0.5 ns and 6 ns after the laser pulse. Chloroplast autofluorescence was acquired using the same excitation wavelength with an acquisition window between 660 and 710 nm using a standard PMT. For all images, scan speed was set at 400 Hz (400 lines s⁻¹) at a resolution at 1024 × 1024 pixels and four lines averaging per single image was used. Fixed DAPI stained images were taken

using default DAPI settings using a 405 nm laser and a detection range of 430–500 nm using a standard PMT. Post-acquisition processing was performed using IMAGEJ1.52p (Rasband, 2018) and assembled in POWERPOINT 2016.

Results

Dek1-tomato^{int} establishment and molecular characterization.

Insertion of a fluorescent tag within a native locus can generate unwanted phenotypes either due to the vector insertion or from the tag itself (Ako *et al.*, 2017). In order to minimize this risk, we adopted the two steps strategy used previously in partial gene deletion in *P. patens* (Demko *et al.*, 2014). The first step consists of the insertion of the construct containing the fluorescent marker and a selection cassette flanked with the pLox sequence using a standard targeted transformation approach. In a second step, the resistance cassette is removed using the transient expression of the Cre recombinase (Trouiller *et al.*, 2006) (Fig. 1a illustrates the three locus states). PEG-mediated protoplast transformation (Cove *et al.*, 2009) of the wild-type (WT) strain using pDEK1-tomato-insertion vector (See Material and methods for vector building) yielded >60 plants (*dek1-pArrowf1s*) displaying a $\Delta dek1$ phenotype (i.e. multiple abortive buds; Perroud *et al.*, 2014). Upon successive genotyping for the loss of the WT locus using the primer pair P-1/P-2, the presence of 5' vector insertion with the primer pair P-3/P-5 and the presence of the vector 3' insertion with the primer pair P-4/P-6 and finally the detection of a single copy of the insert using the primer pair P-3/P-4, three transformants were found to contain a single insertion at the locus. The observed $\Delta dek1$ phenotype indicated that the construct insertion generated a null phenotype potentially caused by the mis-splicing of the modified intron that contained the resistance cassette, a phenomenon observed previously in *Physcomitrella* (Demko *et al.*, 2014; Johansen *et al.*, 2016; Ako *et al.*, 2017). To remove the resistance cassette, we subsequently transiently expressed the Cre recombinase (Trouiller *et al.*, 2006) in protoplasts of the primary transformant *dek1-pArrowf1-1* containing a single insert at the locus. Fifty percent of the picked protoplasts regenerated into plants forming WT-looking gametophores. As predicted by the treatment with Cre recombinase, such gametophore-bearing plants lost hygromycin resistance, too (Fig. S1). Three independent plants were picked randomly and submitted to Southern blot analysis (Fig. S2). They all displayed patterns consistent with the loss of the resistant marker and the presence of a single *tdTomato* sequence at the proper genomic locus. Transformant #1 was chosen and will be referred to as *dek1-tomato^{int}* hereafter. The predicted protein DEK1-TOMATO^{INT} produced in this transgenic strain is illustrated in Fig. 1(b).

Dek1-tomato^{int} impacts upon the *P. patens* life cycle

We followed *Dek1-tomato^{int}* development from regenerating protonema to sporophyte development. Until 14 d of growth on

BCD medium, *dek1-tomato^{int}* was indistinguishable from the WT strain. The protonema differentiates into caulonemal and chloronemal cells and at this time point the number of buds per filament of 15 cells is 1, similar to the WT strain (Fig. S3) and significantly lower than all known *Ppdek1* mutants (Johansen *et al.*, 2016). The growing gametophores develop in a similar way to the WT strain and do not show any of the aberrant growth observed with deletion or insertion in other domains of the *PpDEK1* gene (Johansen *et al.*, 2016). We performed sporophyte induction as described previously (Perroud *et al.*, 2019) and analyzed gametangia development during the fourth week of inductive treatment. No obvious morphological defect was detectable, and both archegonia and antheridia appeared to reach maturity (Fig. S4). The opening of the neck took place in the mature archegonium, similar to the WT (Fig. S4c–h), and the spermatozooids were released from the antheridia. However, we did not detect any sporophyte in five independent trials, either at normal procedure time (after 5 wk of culture in cold conditions), nor after extended culture growth (after 10 and 15 wk of extended culture). In order to evaluate the female fertility of *dek1-tomato^{int}*, we co-cultivated it in the presence of *Vx-red* and *RemCherry*, two efficient *Physcomitrella* male strains (Perroud *et al.*, 2011, 2019). In both cases *dek1-tomato^{int}* remained sporophyteless, indicating that this specific tagging of DEK1 has an effect on the fertility of the female germ line, or on activation of the zygote program. When isolated (Meyberg *et al.*, 2019), *dek1-tomato^{int}*

and Gransden spermatozooids did not show any significant morphological differences (Fig. S5). However, the partially developed spermatozoid appeared more numerous than in the WT strain, potentially indicating that the fluorescent tag may negatively affect spermatogenesis. Testing for male fertility is more challenging, but the recent establishment of a male-specific sterile mutant *ccdc39*, without other apparent defects (Meyberg *et al.*, 2019), allowed us to test *dek1-tomato^{int}* for male fertility. To this effect, we performed a standard crossing assay between *dek1-tomato^{int}* and *ccdc39* in parallel with the control cross Gransden and *ccdc39*. Here, no sporophytes were observed in *ccdc39* with *dek1-tomato^{int}* as the male donor, whereas the control cross trial with Gransden yielded sporophyte on *ccdc39*, both with standard experimental and extended time frames. We conclude that the *dek1-tomato^{int}* spermatozooids were not able to fertilize the *ccdc39* egg cell and hence the tagged Dek1 affects the male germ line. Taken together, these sporulation assays suggest that the tag present in *dek1-tomato^{int}* induces sterility in the male and female gamete proper development or during the fertilization event.

DEK1-TOMATO^{INT} displays a strong subcellular polar distribution from the onset of 3D gametophytic establishment

Dek1-tomato^{int} did not display any signal stronger than background fluorescence using fluorescent microscopy or standard

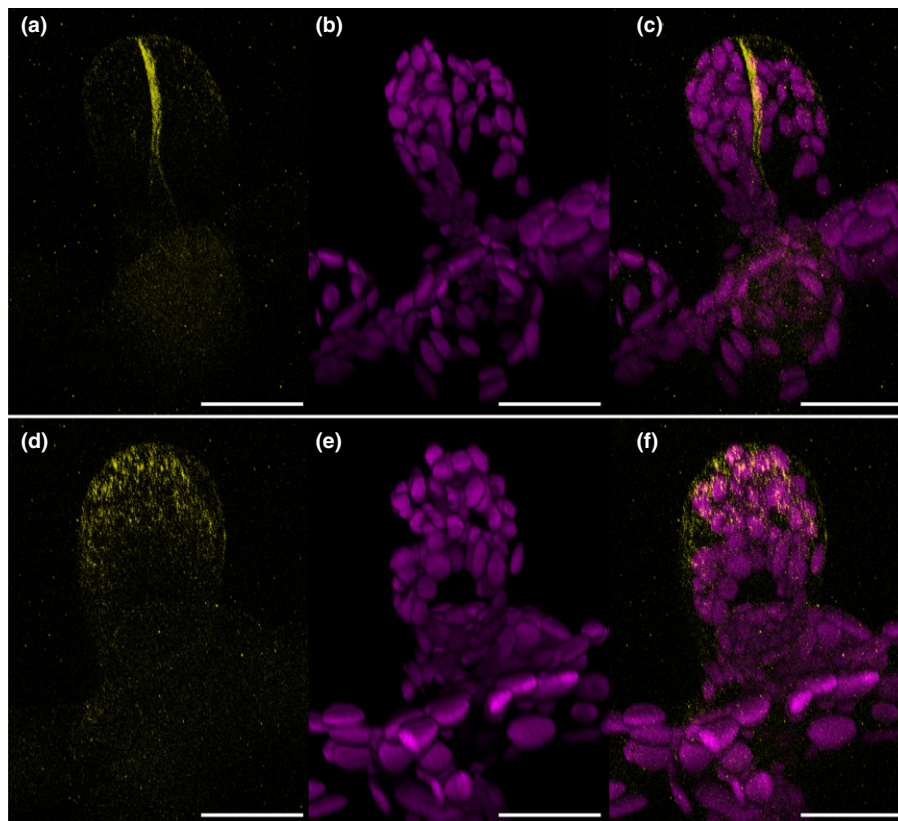


Fig. 2 Tagged Defective Kernel 1 protein DEK1-TOMATO^{INT} is detected at the interface of the first bud cell division in *Physcomitrella patens*. Two-celled bud view perpendicular to (a–c) and facing (d–f) the cell wall separating the two cells: (a, d) DEK1-TOMATO^{INT} specific fluorescent signal; (b, e) Chlorophyll auto-fluorescence specific signal. (c, f) Merged picture with both fluorescent signals. Bars, 20 μ m.

confocal scanning electron microscopy (SEM) techniques. Hence, to detect DEK1-TOMATO^{INT} signal, we used confocal microscopy associated with a time-gating approach (Kodama, 2016) (see the 'Materials and Methods' section for specific parameters). The protonemal tissue (2D growing tissue) did not display any signal, but the first bud cell division (transitional tissue between 2D and 3D growth) showed a low but specific signal (Fig. 2). DEK1-TOMATO^{INT} was detectable at the interface separating the first two cells of the *Physcomitrella* bud. The signal accumulation in the outward face of the two cells was either below the detection limit or absent, but the difference between the two daughter cell faces (adjacent and outward) demonstrates

a strong polarity distribution of DEK1-TOMATO^{INT} in early bud cells. During the subsequent bud cell divisions (Fig. S6), the same signal distribution was observed at each interface of new bud cells. By contrast, faces of the same cells not adjacent to their sister cell continued to be devoid of the above background fluorescent signal. Once the gametophore proper started to develop further (e.g. when phyllids (nonvascular leaves) were morphologically identifiable), a similar signal distribution was observed with a relatively stronger intensity (Fig. 3a–c). This signal remained homogenous during the initial phyllid growth stage (Fig. 3d–f). During this growth phase, the overall higher signal strength allowed the confirmation of a very weak signal in noncontiguous

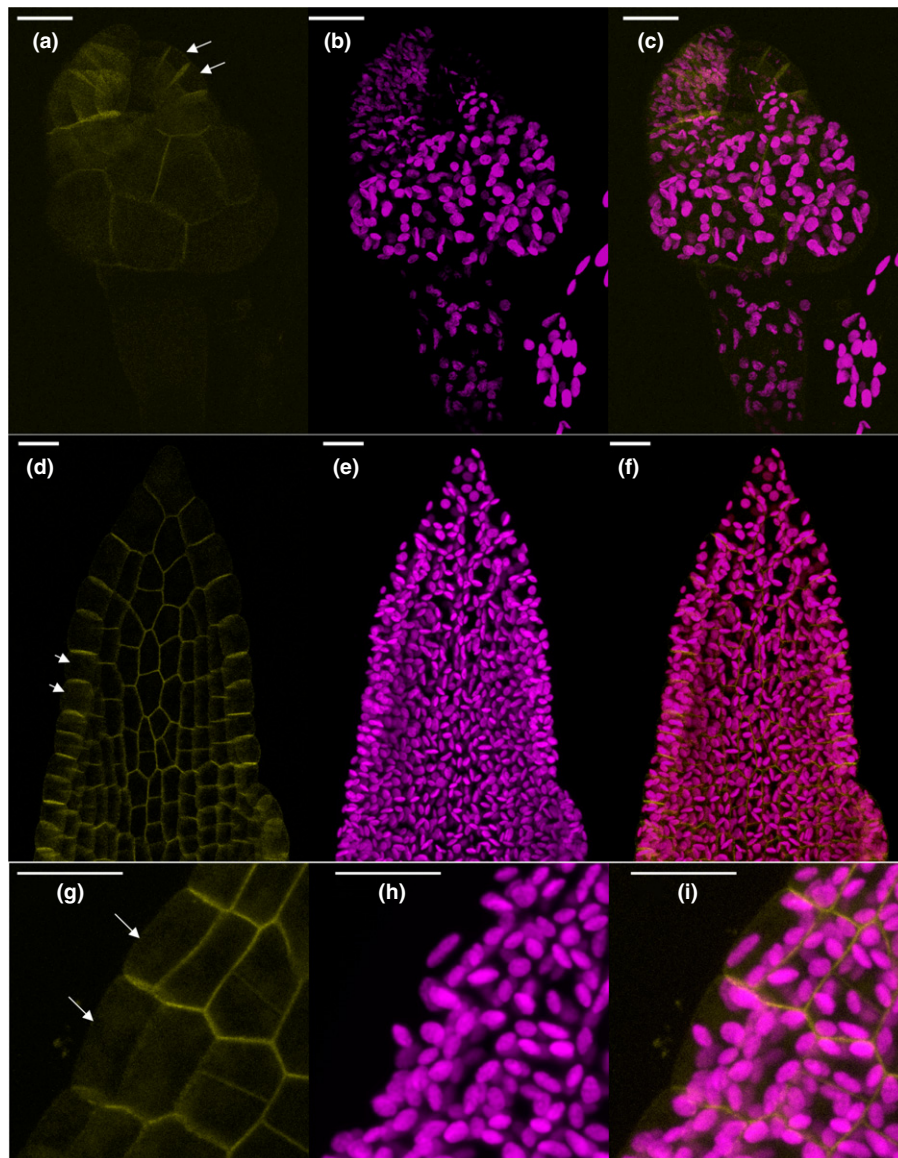


Fig. 3 Tagged Defective Kernel 1 protein DEK1-TOMATO^{INT} localizes at the interface of all growing cells in bud and young phyllids in *Physcomitrella patens*. (a–c) Phyllid cells display a strong asymmetrical DEK1-TOMATO^{INT} fluorescent signal as soon as they are formed in very early gametophores. (d–f) Phyllid cells display a strong asymmetrical DEK1-TOMATO^{INT} fluorescent signal during phyllid formation. (g–i) The signal is easily detectable at the interface of all cells but is low in the cell faces not in contact with their neighbouring cells. White arrows pointing to cell faces at the edge of the phyllid show very low signal accumulation. (a, d, g) DEK1-TOMATO^{INT} specific fluorescent signal. (b, e, h) Chlorophyll auto-fluorescence specific signal. (c, f, i) Merged picture with both fluorescent signals. Bars, 20 μ m.

cell faces in this tissue (Fig. 3g–i). Additionally, the signal in this tissue confirmed the plasma membrane DEK1 localization. As the plasma membrane retracts upon osmolyte treatment, the signal strength drops rapidly and the remaining signal stays associated with the plasma membrane leaving a cell wall free of fluorescent signal (Fig. S7).

DEK1-TOMATO^{INT} detection is associated specifically with developing tissue

As the phyllid grew, the DEK1-TOMATO^{int} polarized signal displayed a decreasing gradient from the base of the phyllid where cells are still dividing and elongating actively, to the tips of the phyllid where cells have a reduced overall growth activity (Fig. 4a–c). When the phyllid has fully developed, when it reached its maximum size, regardless of its position on the gametophore, the polarized signal disappeared completely to a diffuse signal indistinguishable from the background (Fig. S8). The DEK1-TOMATO^{INT} asymmetrical cell distribution and its organ developmental pattern (the clear signal in actively growing cell, and the loss of the signal in cells of mature organ) also were observed during gametangia development. Both developing archegonia (Fig. 5e–f) and developing antheridia (Fig. 5j–l) cells displayed similar strong asymmetrical signal distribution observed in phyllid cells. In the case of the archegonia, this signal vanished completely at the opening of the fertilization (neck) canal (Fig. 5g–l). Male gamete development leads to the formation of the single-celled motile spermatozoid in which the DEK1-TOMATO^{INT} signal is different. During the growing antheridium phase, the DEK1-TOMATO^{INT} signal initially was similar to the other gametophytic tissues: a polar accumulation at the interface of two divided cells. But as spermatozoid differentiation started, DEK1-TOMATO^{INT} disappeared from the antheridium jacket cells and a strong signal was detectable in the developing spermatozoid (Fig. 5m–o). As spermatogenesis was initiated, the DEK1-TOMATO^{INT} signal was first observable as a large dot when the antheridium reaches the developmental stage 7 (Landberg *et al.*, 2013) and remained strong as the spermatozoid differentiated into their final fasciculate shape, during stages 8 and 9 of antheridium development (Figs 5m–o, S9). Upon spermatozoid release in water the signal vanished rapidly.

PpDEK1 does not require an active calpain to localize at the initial cell bud division

In order to evaluate the importance of the calpain activity in the localization of DEK1, we generated the specific single-codon replacement mutant *dek1*^o (Johansen *et al.*, 2016) in the *dek1-tomato^{int}* background. This mutation is situated in the active site of the DEK1-Calpain domain where the Cys-1782 is replaced by a Ser, produces a Δ *dek1* null phenotype, but leaves a mutated full transcript in the plant. *Dek1-tomato^{int}/dek1^o* was established by transforming the *dek1-tomato^{int}* strain with the vector pArrow-DEK1^o (Fig. S10) as performed previously (Johansen *et al.*, 2016). The *Dek1-tomato^{int}* protoplast yield and appearance were similar to those of WT origin and the transformation yielded

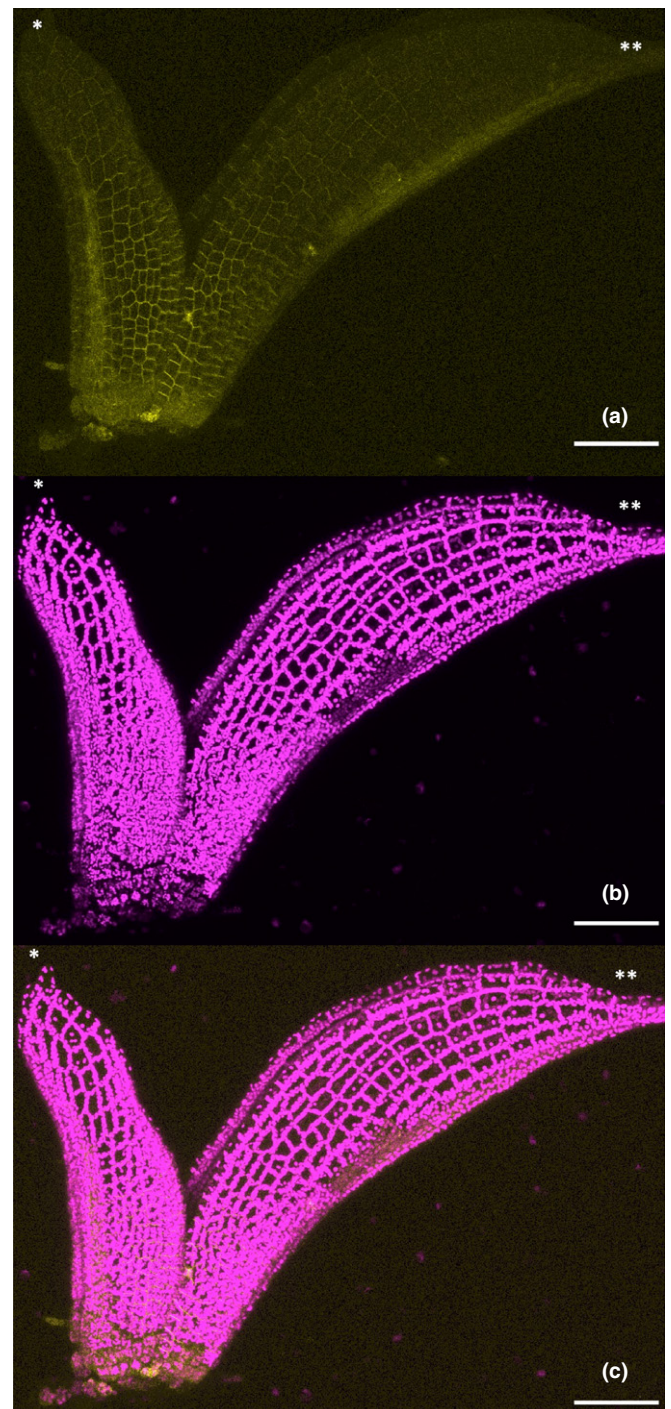


Fig. 4 Tagged Defective Kernel 1 protein DEK1-TOMATO^{INT} polarized signal fades away as phyllid cells of *Physcomitrella patens* reach maximum size. At the base of both phyllids a strong signal is observed in all cells as they divide and elongate. The polarized signal is easily detectable up to the tip of left (younger and shorter phyllid) (*) and already is totally diffuse at the tip of the older and larger phyllid (**). (a) DEK1-TOMATO^{INT} specific fluorescent signal. (b) Chlorophyll auto-fluorescence specific signal. (c) Merged picture with both fluorescent signals. Bars, 10 μ m.

multiple transformants displaying the previously observed *dek1*^o (abortive buds). The PCR genotyping performed on three such transformants using primers designed outside of the targeted locus confirmed the 5' and 3' proper insertion of the vector

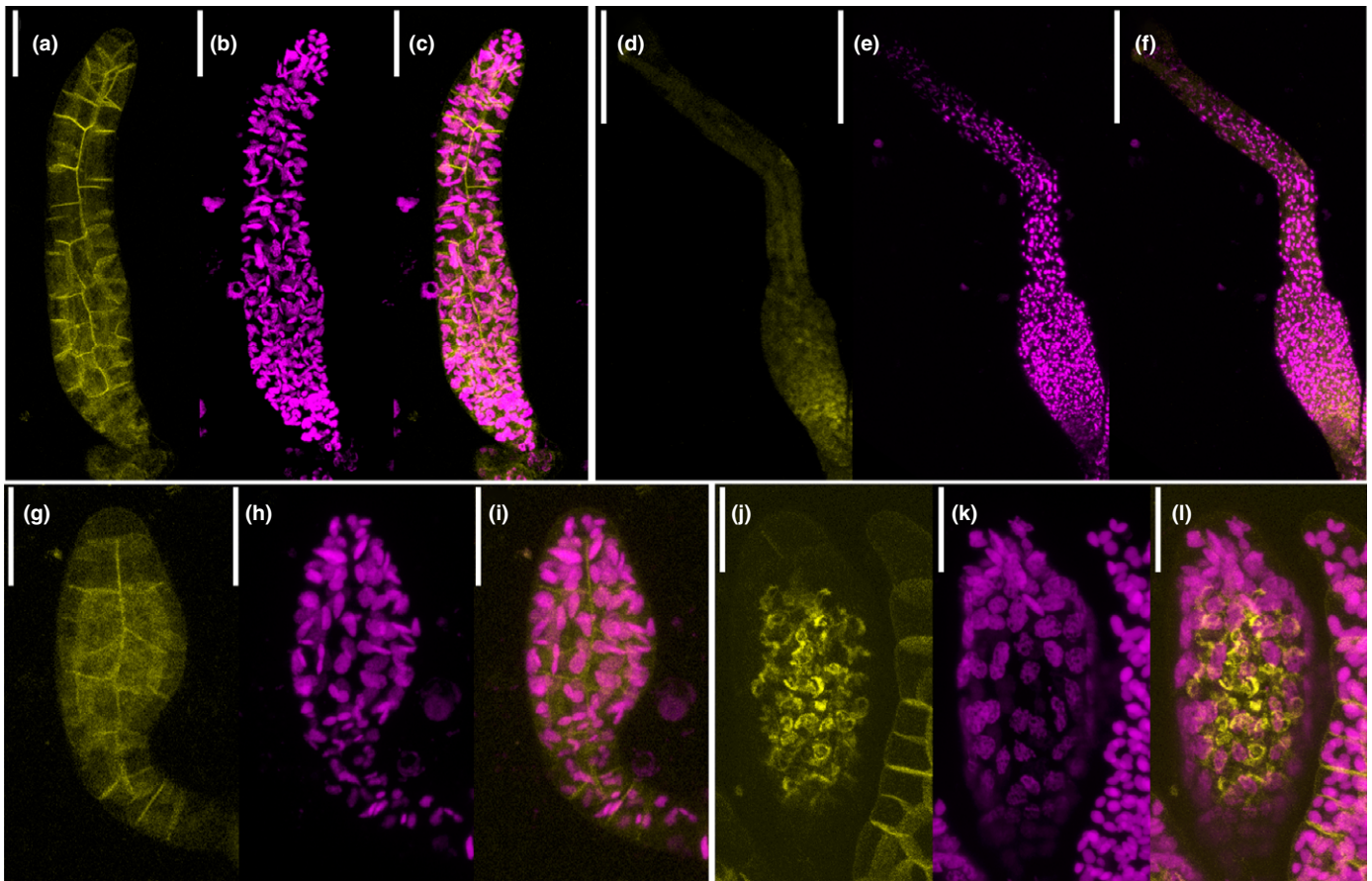


Fig. 5 Tagged Defective Kernel 1 protein DEK1-TOMATO^{INT} during gametangia development of *Physcomitrella patens*. (a–c) The developing archegonium (female gametangium) is displaying DEK1-TOMATO^{INT} signal at the interface of dividing cell. Bars, 10 μ m. (d–f) Mature archegonium (fertilization canal opened) is displaying a very low diffuse DEK1-TOMATO^{INT} signal. Bars, 20 μ m. (g–i) A developing antheridium (male gametangium) is displaying DEK1-TOMATO^{INT} signal at the interface of dividing cell. Bars, 20 μ m. (j–l): In closed mature antheridium before spermatozoid release the DEK1-TOMATO^{INT} polarized signal in the antheridial jacket is almost gone but a strong signal is present in individual spermatozoids. For comparison, see the DEK1-TOMATO^{INT} in the edge of a young phyllid on the right side of the image. Bars, 20 μ m. (a, d, g, j) DEK1-TOMATO^{INT} specific fluorescent signal. (b, e, h, k) Chlorophyll auto-fluorescence specific signal. (c, f, i, l) Merged picture with both fluorescent signals.

(Fig. S10b). Furthermore, sequencing of the RT-PCR fragment performed on the three transformants confirmed the presence of the mutated site in the transcript (Figs S11a,b, S12). Transformant #2 was chosen as representative strain and is referred to hereafter as *dek1-tomato^{int}/dek1^o*. A final RT-PCR performed with a primer pair flanking the *tdTomato* sequence confirmed the presence of the fluorophore sequence in *dek1-tomato^{int}/dek1^o* *Dek1* transcript (Fig. S11c). In addition to the absence of developing leafy gametophore of *dek1-tomato^{int}/dek1^o*, the comparison between the WT strain, *dek1-tomato^{int}* and *dek1-tomato^{int}/dek1^o* confirmed the overabundance of budding events in *dek1-tomato^{int}/dek1^o*, as observed previously in Δ *dek1* and *dek1^o* (Perroud *et al.*, 2014; Johansen *et al.*, 2016) (Fig. S3). The DEK1-TOMATO^{INT} fluorescent signal in *dek1-tomato^{int}/dek1^o* emerging two-celled bud, observed between 7 and 9 d after culture inoculation, displayed a low signal similar to that detected in *dek1-tomato^{int}* (Fig. 6a–c) indicating that if the codon change generated abortive gametophores, it did not affect the DEK1 localization upon bud initiation. In older buds observed between 10 and 14 d post-inoculation, the signal was still detectable

between the most recently divided cells but appeared to fade in the oldest cells of the bud (Fig. 6d–f). Additionally, some multi-celled buds observed at the same time point completely lost the polarized signal (Fig. 6g–i). Overall, the signal seems present between recently divided bud cells but vanishes as the bud undergoes mitotic arrest. Apparently, an active calpain is not necessary to localize DEK1 at the interface of the first bud cell division, but is required for the maintenance of such signal and the further establishment of the gametophore.

Discussion

The detection of Defective Kernel 1 (DEK1) using fluorescent protein tagging in a native expression context was successful and revealed two main notable distribution features in 3D developing tissue. DEK1 displays a strong polarized subcellular distribution in cells of 3D developing tissues (Fig. 3) and shows a specific developmental pattern linked to tissue growth both in terms of cell division and cell elongation (Figs 4, 5). Localization of the tagged Defective Kernel 1 protein DEK1-TOMATO^{INT} at the

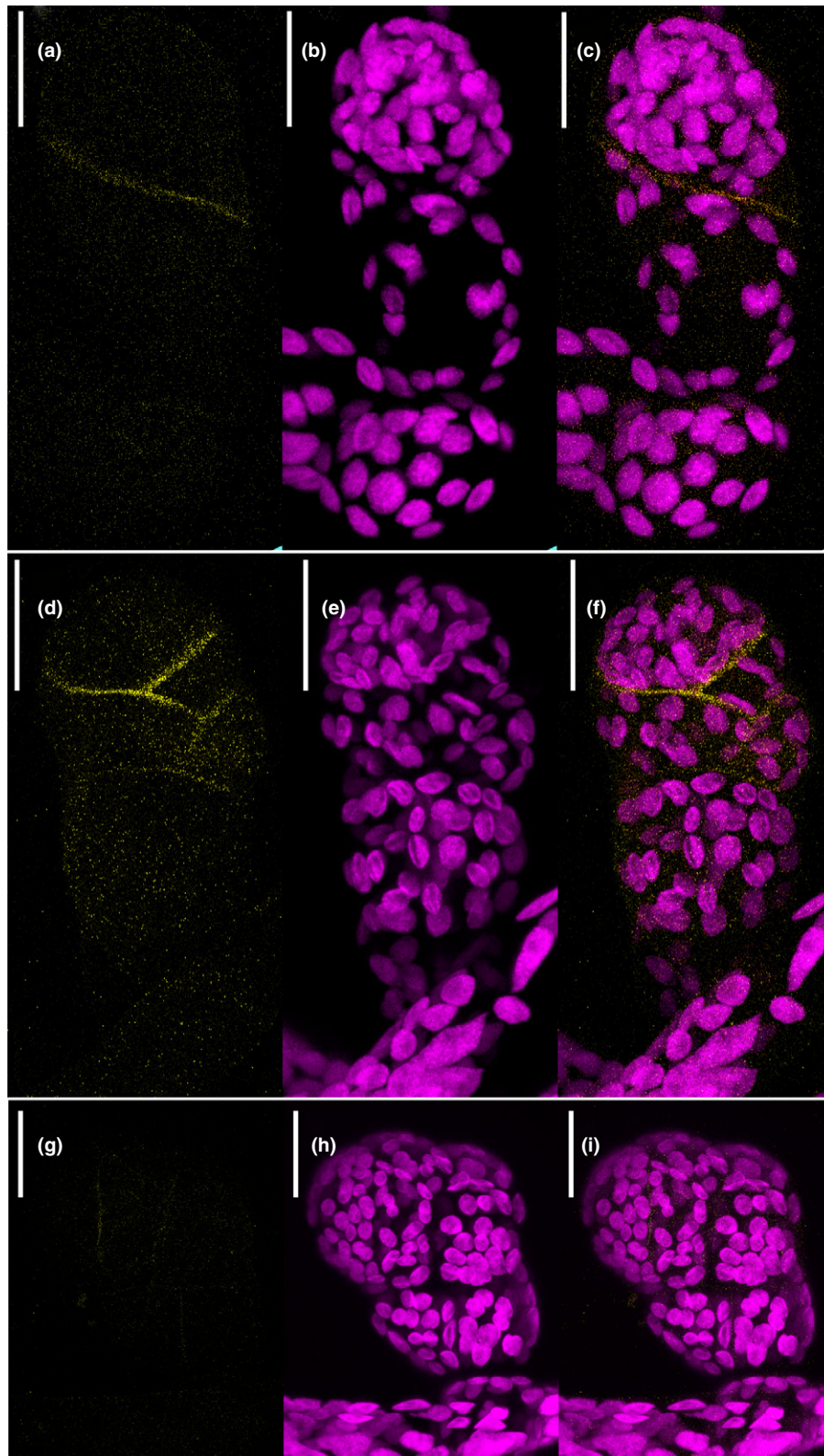


Fig. 6 Tagged Defective Kernel 1 protein DEK1-TOMATO^{INT} signal is detected in *dek1-tomato^{int}/dek1^o* *Physcomitrella patens* plant. (a–c) A two-celled bud displays DEK1-TOMATO^{INT} signal at the interface of divided cell. (d–f) A five-celled bud displays DEK1-TOMATO^{INT} signal at the interface of recently divided cells, whereas older cells display a reduced DEK1-TOMATO^{INT} signal. (g–i) A five-celled bud displays no detectable DEK1-TOMATO^{INT} signal. (a, d, g) DEK1-TOMATO^{INT} specific fluorescent signal. (b, e, h) Chlorophyll auto-fluorescence specific signal. (c, f, i) Merged picture with both fluorescent signals. Bars, 20 μ m.

plasma membrane matches both the structural prediction based on the primary amino acid sequence (Lid *et al.*, 2002) and the previous detection in *Arabidopsis* (Johnson *et al.*, 2008) and in *Physcomitrella* (Perroud *et al.*, 2014). However, its asymmetrical localization at the face of recently divided cells of 3D tissue is new and can probably only be observed due to the sensitive *in locus* tagging approach used here.

A polarized signal is in accordance with the functional model (Tian *et al.*, 2007; Gruis *et al.*, 2006), which proposes that DEK1 is responsible for the perception of tissue boundaries in land plants. In the relatively simple gametophores model system, contiguous cell sides are considered as the inner side of the tissue with all cell sides free of cell contact being the outer side. DEK1 detection at the interface of cells rather than at the outside indicates that DEK1 function could be the integration of neighbouring cell presence as primary cue, rather than perceiving the outer boundary of a tissue *per se*. In a second step, the cell could interpret the polarization (or lack thereof for internal cells) directly through calpain activity and its interaction with other proteins to trigger specific developmental steps. The initial DEK1 localization could be developmental by nature: once the bud developmental program is initiated, the DEK1 is targeted and stabilized at the cell plate during mitosis, where its accumulation leads to the observed signal. The question which arises then is: What conveys DEK1 localization at the interface of the two dividing cell in developing 3D tissue? We show clearly that calpain activity is not necessary to initiate DEK1 localization (Fig. 6) and furthermore the successful complementation experiments with solely the calpain domain (Johnson *et al.*, 2008; Johansen *et al.*, 2016) indicate that calpain polarity is not necessary to fulfill activated calpain domain function. Hence the polarity factor lies most likely in the DEK1-MEM (membrane) domain. One or multiple external MEM subdomains linking its many transmembrane spans could act as linker(s) to parietal compounds present at cell plate deposition. The effect of deletion of the largest Loop domain (Demko *et al.*, 2014) pleads for a complex interaction, as in this case, in which the bud development is not arrested but the development of the phyllid is. Alternatively, DEK1 localization could be triggered actively through local mechanisms such as mechanosensing (Tran *et al.*, 2017). DEK1 would perceive the difference between the mechanical properties in the outer cell wall and the intercalary cell wall, and accumulate only in the latter. Another potential local variable that DEK1 could integrate is the differential solute composition and/or concentration between apoplast and outer boundary tissue limit. The recently isolated Nucleolar G-protein *nog1* mutant (Moody *et al.*, 2018) may give a clue for a nonexclusive alternative to explain DEK1 polarity distribution: targeted protein degradation. *Nog1* phenotype displays abortive buds identical to those of $\Delta dek1$, and similar to the complementation of $\Delta dek1$ by cDNA overexpression (Perroud *et al.*, 2014) shows overall reduction (or a delay) of bud initiation events (Moody *et al.*, 2018). In a similar way to DEK1, the specific structure of NOG1 protein is highly conserved in land plants and its transcript is present in all observed tissues (Moody *et al.*, 2018). The protein NOG1 contains a well-defined ubiquitin domain that targets bound proteins to the 26S proteasome for degradation that led to a multi-target indirect

protein degradation model to explain the effect of NOG1 mutation in *Physcomitrella* (Moody *et al.*, 2018). Retaining the NOG1 protein degradation hypothesis, a direct interaction model between DEK1 and NOG1 could explain the observed DEK1 polarity and its effect on bud formation. When DEK1 is associated with the recently divided cell wall it is protected from the PpNOG1-mediated degradation process, as any DEK1 delivered to the outer cell wall domain will be targeted for degradation, leading to the polar DEK1-TOMATO^{int} signal that we observe. The DEK1 polarity observed is thus necessary for bud development not only through the regulation of DEK1-calpain activity, but also to control the MEM-DEK1 domain abundance as its overexpression alone leads to aberrant plant development (Tian *et al.*, 2007). As cells elongate and age in the developing tissue, the protection initially conferred at cell division is reduced and ultimately goes away, and DEK1 become target of the degradation process that leads to the observed DEK1-TOMATO^{int} signal developmental pattern. This model of the interaction between DEK1 and NOG1 also would explain the bud number change observed in the protonema with their respective mutants. The absence of NOG1 would increase DEK1 abundance that results in observed reduced number of bud initiation (Moody *et al.*, 2018), the opposite phenotype observed in $\Delta dek1$ where the over-budding is detected. Concordantly, the complementation of $\Delta dek1$ by its cDNA overexpression (Perroud *et al.*, 2014) displays a delayed gametophore initiation and development. Such cell polarity maintenance through modulation of protein degradation is a phenomenon observed in other eukaryotic organisms (Bórquez & González-Bilbault, 2011). For example, in zebrafish the protein Retinitis Pigmentosa GTPase Regulator-Interacting Protein 1-like prevents dishevelled degradation and maintains planar polarity (Mahuzier *et al.*, 2012) and in mammalian epithelial cells, the serine/threonine kinase salt inducible kinase 1-mediated targeting of the polarity determinant like-polarity complex protein 3 leads to protein degradation and cell polarity loss (Vanlandewijck *et al.*, 2018).

In the *dek1^o* background, DEK1-TOMATO^{int} localizes properly at the onset of the bud formation but the signal fades within three to five days leading to an arrested bud. The observation of DEK1-TOMATO^{int} signal reduction over time either with tissue development in *dek1-tomato^{int}* where mature tissue does not display any signal or at bud arrest in *dek1-tomato^{int}/dek1^o*, underlines the link between DEK1 and the cell cycle. In both cases, next to no cell divisions are observed, but the tissue remains viable for an extended period of time. Indeed, not only are mature phyllids still photosynthetically active, a function necessary for future sporophyte development (Regmi *et al.*, 2017), but also their developmental program can be redirected toward protonemal faith upon wounding signal for example (Ishikawa *et al.*, 2011), a tissue that does not require DEK1 for its growth.

The DEK1-TOMATO^{int} subcellular localization and developmental pattern distribution are reminiscent of the PINFORMED (PIN) proteins, well-described auxin efflux carriers (Bennett, 2015), in the gametophore. Immunolocalization of PINA and PINB in young phyllids revealed a similar polarized signal, with the signal essentially detected at the interface of cell,

leaving the outer cell face free of signal (Bennett *et al.*, 2014). *In vivo* detection of the same proteins using green fluorescent protein (GFP) fusion tagging depicted a similar picture but revealed difference with DEK1-TOMATO^{int} (Viaene *et al.*, 2014). First, the signal for these proteins was detected at high level in protonema filament, in which DEK1 is not observed. However, PINs are absent from early buds and only become apparent after the initiation of phyllid development. In phyllids the developmental signal is divergent: as DEK1 vanished as soon as phyllid maximum cell size was achieved, PINA or PINB remained visible in adult phyllids for longer time. Additionally signal polarity appeared to be lost near the base of the phyllid, even as the PIN signal remains detectable at the plasma membrane. It is of note that even if the double knockout (KO) of these genes affects phyllid morphological development, this mutant remains fertile notwithstanding that sporophyte development is strongly affected (Bennett *et al.*, 2014; Viaene *et al.*, 2014). Unfortunately the triple KO *PpPINABC* is apparently lethal as no viable tissue could be recovered, so the potential impact of the absence of plasma membrane PIN on 3D growth could not be evaluated (Viaene *et al.*, 2014). In any case the similar co-occurrence of DEK1 and PINs indicates a potential common function in 3D growth establishment that would directly link DEK1 to auxin-controlled growth mechanisms. Alternatively, both protein types may use similar cues to localize during gametophore development. Other membrane-bound proteins such as *PpCLAVATA* and *PpRPK2* recently have been shown to be involved in gametophore development (Whitewoods *et al.*, 2018). Their exact cellular localization remains unknown and their mutations lead to clear meristematic activity disorganization in gametophore, mirroring their meristem maintenance function in angiosperms. But phyllid development remains present in their mutants, suggesting that their biological function is downstream of DEK1. However, they could interact with DEK1 at the plasma membrane to perform their developmental function.

The detection of *DEK1-tomato^{int}* in the male germ line during spermatogenesis is novel in plants. However, the presence of calpain in mammals in sperm/testis is well-described. Multiple calpains are present during this developmental phase as well as in fully formed sperm cells (Schollmeyer, 1986; Macqueen & Wilcox, 2014). Additionally, one classical calpain, CAP11 appears to be expressed and accumulated specifically during spermatogenesis in spermatozooids in human and mouse testes (Dear *et al.*, 1999; Ben-Aharon *et al.*, 2006). Involvement of calpains in cytoskeleton rearrangement during sperm cell development (Ben-Aharon *et al.*, 2006), in acrosome function (Schollmeyer, 1986), as well as during fertilization events (Rojas & Moretti-Rojas, 2000) have been proposed for these calpains, although they remain to be demonstrated. Calpains also have been associated with protozoan motile cells, such as CALP1.3 with flagellum of *Trypanosoma brucei* (Liu *et al.*, 2010). DEK1 could be the bearer of such functions in land plant motile gametes. In plants, there is no reason to postulate a different DEK1 molecular activity function between spermatozooids and gametophore cells. But, the biological context, the differentiation of a unicellular cell motile type by opposition to the 3D gametophore growth, suggests that the

signal DEK1 perceives as well as the downstream regulatory network it influences may be different. At the phenotypic level, the strong signal during spermatogenesis may hint at the cause of the male sterility observed in crossing trial. We ruled out that the absence of a sporophyte could be attributed to the well-documented low male fertility of the Gransden strain in general (Perroud *et al.*, 2011, 2019; Landberg *et al.*, 2013; Ashton & Raju, 2014; Hiss *et al.*, 2017; Meyberg *et al.*, 2019). However, it is possible that vegetative amplification of *dek1-tomato^{int}* for several years led to a sterility problem. Future investigation in fully fertile background *Physcomitrella* ecotypes such as Villersexel (Perroud *et al.*, 2011) or Reute (Hiss *et al.*, 2017) may help refine these observations. However, the presence of the tag in the protein may be causing this spermatozoid sterility. The observed signal may reflect a specific function in spermatogenesis that the tag deregulates by stabilizing or destabilizing the DEK1 protein in this context, as cellular processes in general can be potentially affected by a fluorescent tag presence (Weill *et al.*, 2019; Ansari *et al.*, 2016). Why *dek1-tomato^{int}* displays such a sterility defect remains an open question as it could be attributed to female and/or male gametogenesis or potentially to the fertilization event.

Acknowledgements

The authors warmly thank Regine Kahmann and Stefanie Reißmann for the generous access to the confocal microscopy equipment at the Max Planck Institute for Terrestrial Microbiology. This project was partially funded by grant FRIMEDBIO 240343 from the Norwegian Research Council to O-AO. VD was supported by the Slovak Research and Development Agency through grant APVV-17-0570.

Author contributions

P-FP and O-AO conceptualized the study; P-FP, VD and RM carried out investigations; P-FP performed the confocal microscopy imaging and assembled the figures; P-FP wrote the original draft, which was reviewed and edited by VD, RM, RSQ, O-AO and SAR; O-AO and VD acquired funding; RSQ, O-AO and SAR collected resources; and O-AO and SAR supervised the research.

ORCID

Viktor Demko  <https://orcid.org/0000-0002-9473-4886>
Rabea Meyberg  <https://orcid.org/0000-0002-9977-4000>
Odd-Arne Olsen  <https://orcid.org/0000-0002-8787-1057>
Pierre-François Perroud  <https://orcid.org/0000-0001-7607-3618>
Ralph S. Quatrano  <https://orcid.org/0000-0003-0371-4415>
Stefan A. Rensing  <https://orcid.org/0000-0002-0225-873X>

References

- Ako AE, Perroud P-F, Innocent J, Demko V, Olsen O-A, Johansen W. 2017. An intragenic mutagenesis strategy in *Physcomitrella patens* to preserve intron splicing. *Scientific Reports* 7: 5111.

- Amanda D, Doblin MS, Galletti R, Bacic A, Ingram GC, Johnson KL. 2016. DEFECTIVE KERNEL1 (DEK1) Regulates cell walls in the leaf epidermis. *Plant Physiology* 172: 2204–2218.
- Ansari AM, Ahmed AK, Matsangos AE, Lay F, Born LJ, Marti G, Harmon JW, Sun Z. 2016. Cellular GFP toxicity and immunogenicity: potential confounders in *in vivo* cell tracking experiments. *Stem Cell Reviews and Reports* 12: 553–559.
- Arthur JSC, Gauthier S, Elce JS. 1995. Active site residues in m-calpain: identification by site-directed mutagenesis. *FEBS Letters* 368: 397–400.
- Ashton NW, Raju MVS. 2014. The distribution of gametangia on gametophores of *Physcomitrella (Aphanogema) patens* in culture. *Journal of Bryology* 22: 9–12.
- Becraft PW, Li K, Dey N, Asuncion-Crabb Y. 2002. The maize dek1 gene functions in embryonic pattern formation and cell fate specification. *Development* 129: 5217–5225.
- Ben-Aharon I, Brown PR, Shalgi R, Eddy EM. 2006. Calpain 11 is unique to mouse spermatogenic cells. *Molecular Reproduction and Development* 73: 767–773.
- Bennett T. 2015. PIN proteins and the evolution of plant development. *Trends in Plant Science* 20: 498–507.
- Bennett TA, Liu MM, Aoyama T, Bierfreund NM, Braun M, Coudert Y, Dennis RJ, O'Connor D, Wang XY, White CD *et al.* 2014. Plasma membrane-targeted PIN proteins drive shoot development in a moss. *Current Biology* 24: 2776–2785.
- Bórquez DA, González-Billault C. 2011. Regulation of cell polarity by controlled proteolytic systems. *Biological Research* 44: 35–41.
- Cove DJ, Perroud P-F, Charron AJ, McDaniel SF, Khandelwal A, Quatrano RS. 2009. The moss *Physcomitrella patens*: a novel model system for plant development and genomic studies. *Cold Spring Harbor Protocols* 4: 69–104.
- Dear TN, Möller A, Boehm T. 1999. CAPN11: A calpain with high mRNA levels in testis and located on chromosome 6. *Genomics* 59: 243–247.
- Demko V, Perroud P-F, Johansen W, Delwiche CF, Cooper ED, Rempe P, Ako AE, Kugler KG, Mayer KFX, Quatrano R *et al.* 2014. Genetic analysis of DEFECTIVE KERNEL1 Loop function in three-dimensional body patterning in *Physcomitrella patens*. *Plant Physiology* 166: 903–919.
- Gruis D (Fred), Guo H, Selinger D, Tian Q, Olsen O-A. 2006. Surface position, not signaling from surrounding maternal tissues, specifies aleurone epidermal cell fate in maize. *Plant Physiology* 141: 898–909.
- Guerrigue Y, Thomine S, Frachisse JM. 2018. Sensing and transducing forces in plants with MSL10 and DEK1 mechanosensors. *FEBS Letters* 592: 1968–1979.
- Hamilton ES, Schlegel AM, Haswell ES. 2015. United in Diversity: Mechanosensitive ion channels in plants. *Annual Review of Plant Biology* 66: 113–137.
- Harrison JC. 2017. Development and genetics in the evolution of land plant body plans. *Philosophical Transactions of the Royal Society of London. Series B: Biological Sciences* 372: 20150490.
- Hibara K-I, Obara M, Hayashida E, Abe M, Ishimaru T, Satoh H, Itoh J-I, Nagato Y. 2009. The ADAXIALIZED LEAF1 gene functions in leaf and embryonic pattern formation in rice. *Developmental Biology* 334: 345–354.
- Hiss M, Meyberg R, Westermann J, Haas FB, Schneider L, Schallenberg-Rüdinger M, Ullrich KK, Rensing SA. 2017. Sexual reproduction, sporophyte development and molecular variation in the model moss *Physcomitrella patens*: introducing the ecotype Reute. *The Plant Journal* 90: 606–620.
- Hosfield CM, Elce JS, Davies PL, Jia Z. 1999. Crystal structure of calpain reveals the structural basis for Ca²⁺-dependent protease activity and a novel mode of enzyme activation. *EMBO Journal* 18: 6880–6889.
- Ishikawa M, Murata T, Sato Y, Nishiyama T, Hiwatashi Y, Imai A, Kimura M, Sugimoto N, Akita A, Oguri Y *et al.* 2011. *Physcomitrella* cyclin-dependent kinase A links cell cycle reactivation to other cellular changes during reprogramming of leaf cells. *The Plant Cell* 23: 2924–2938.
- Johansen W, Ako AE, Demko V, Perroud P-F, Rensing SA, Mekhlif AK, Olsen O-A. 2016. The DEK1 calpain linker functions in three-dimensional body patterning in *Physcomitrella patens*. *Plant Physiology* 172: 1089–1104.
- Johnson KL, Degnan KA, Ross Walker J, Ingram GC. 2005. AtDEK1 is essential for specification of embryonic epidermal cell fate. *The Plant Journal* 44: 114–127.
- Johnson KL, Faulkner C, Jeffree CE, Ingram GC. 2008. The phyto-calpain defective kernel 1 is a novel *Arabidopsis* growth regulator whose activity is regulated by proteolytic processing. *The Plant Cell* 20: 2619–2630.
- Kodama Y. 2016. Time gating of chloroplast autofluorescence allows clearer fluorescence imaging in *planta*. *PLoS ONE* 11: e0152484.
- Landberg K, Pederson ERA, Viaene T, Bozorg B, Friml J, Jönsson H, Thelander M, Sundberg E. 2013. The moss *Physcomitrella patens* reproductive organ development is highly organized, affected by the two SHI/STY genes and by the level of active auxin in the SHI/STY expression domain. *Plant Physiology* 162: 1406–1419.
- Lang D, Saleh O, Decker EL, van Gessel N, Hoernstein SNW, Zimmer AD, Reski R, Gundlach H, Mayer KFX, Ullrich KK *et al.* 2018. The *Physcomitrella patens* chromosome-scale assembly reveals moss genome structure and evolution. *The Plant Journal* 93: 515–533.
- Liang Z, Demko V, Wilson RC, Johnson KA, Ahmad R, Perroud P-F, Quatrano R, Zhao S, Shalchian-Tabrizi K, Otegui MS *et al.* 2013. The catalytic domain CysPc of the DEK1 calpain is functionally conserved in land plants. *The Plant Journal* 75: 742–754.
- Lid SE, Gruis D, Jung R, Lorentzen JA, Ananiev E, Chamberlin M, Niu X, Meeley R, Nichols S, Olsen O-A. 2002. The defective kernel 1 (dek1) gene required for aleurone cell development in the endosperm of maize grains encodes a membrane protein of the calpain gene superfamily. *Proceedings of the National Academy of Sciences, USA* 99: 5460–5465.
- Lid SE, Olsen L, Nestestog R, Aukerman M, Brown RC, Lemmon B, Mucha M, Opsahl-Sorteberg HG, Olsen O-A. 2005. Mutation in the *Arabidopsis thaliana* DEK1 calpain gene perturbs endosperm and embryo development while over-expression affects organ development globally. *Planta* 221: 339–351.
- Liu W, Apagy K, McLeavy L, Ersfeld K. 2010. Expression and cellular localisation of calpain-like proteins in *Trypanosoma brucei*. *Molecular and Biochemical Parasitology* 169: 20–26.
- Macqueen DJ, Wilcox AH. 2014. Characterization of the definitive classical calpain family of vertebrates using phylogenetic, evolutionary and expression analyses. *Open Biology* 4: 130219.
- Mahuzier A, Gaudé HM, Grampa V, Anselme I, Silbermann F, Leroux-Berger M, Delacour D, Ezan J, Montcouquiol M, Saunier S *et al.* 2012. Dishevelled stabilization by the ciliopathy protein rpgrip11 is essential for planar cell polarity. *Journal of Cell Biology* 198: 927–240.
- Malivert A, Hamant O, Ingram G. 2018. The contribution of mechanosensing to epidermal cell fate specification. *Current Opinion in Genetics and Development* 51: 52–58.
- Meyberg R, Perroud P-F, Haas F, Schneider L, Heimerl T, Renzaglia K, Rensing SA. 2019. Characterization of evolutionarily conserved key players affecting eukaryotic flagellar motility and fertility using a moss model. *bioRxiv*: 728691.
- Moody LA. 2019. The 2D to 3D growth transition in the moss *Physcomitrella patens*. *Current Opinion in Plant Biology* 47: 88–95.
- Moody LA, Kelly S, Rabinowitsch E, Langdale JA. 2018. Genetic regulation of the 2D to 3D growth transition in the moss *Physcomitrella patens*. *Current Biology* 28: 473–478.
- Olsen O-A, Perroud P-F, Johansen W, Demko V. 2015. DEK1; missing piece in puzzle of plant development. *Trends in Plant Science* 20: 70–71.
- Omasits U, Ahrens CH, Müller S, Wollscheid B. 2014. Protter: interactive protein feature visualization and integration with experimental proteomic data. *Bioinformatics* 30: 884–886.
- Ono Y, Sorimachi H. 2012. Calpains – an elaborate proteolytic system. *Biochimica et Biophysica Acta - Proteins and Proteomics* 1824: 224–236.
- Perroud P-F, Cove DJ, Quatrano RS, McDaniel SF. 2011. An experimental method to facilitate the identification of hybrid sporophytes in the moss *Physcomitrella patens* using fluorescent tagged lines. *New Phytologist* 191: 301–306.
- Perroud P-F, Demko V, Johansen W, Wilson RC, Olsen O-A, Quatrano RS. 2014. Defective Kernel 1 (DEK1) is required for three-dimensional growth in *Physcomitrella patens*. *New Phytologist* 203: 794–804.
- Perroud P-F, Meyberg R, Rensing SA. 2019. *Physcomitrella patens* Reute mCherry as a tool for efficient crossing within and between ecotypes. *Plant Biology* 21: 143–149.

- Perroud P-F, Quatrano RS. 2006. The role of ARPC4 in tip growth and alignment of the polar axis in filaments of *Physcomitrella patens*. *Cell Motility and the Cytoskeleton* 63: 162–171.
- Qu X, Chatty PR, Roeder AHK. 2014. Endomembrane trafficking protein SEC24A regulates cell size patterning in *Arabidopsis*. *Plant Physiology* 166: 1877–1890.
- Rasband W. 2018. *ImageJ 1997–2018*. Bethesda, MD, USA: US National Institutes of Health. [WWW document] URL <https://imagej.nih.gov/ij/>.
- Regmi KC, Li L, Gaxiola RA. 2017. Alternate modes of photosynthate transport in the alternating generations of *Physcomitrella patens*. *Frontiers in Plant Science* 8: 1956.
- Resing SA. 2018. Great moments in evolution: the conquest of land by plants. *Current Opinion in Plant Biology* 42: 49–54.
- Rojas FJ, Moretti-Rojas I. 2000. Involvement of the calcium-specific protease, calpain, in the fertilizing capacity of human spermatozoa. *International Journal of Andrology* 23: 163–168.
- Schaefer DG, Delacote F, Charlot F, Vrielynck N, Guyon-Debast A, Le Guin S, Neuhaus J-M, Doutriaux MP, Nogué F. 2010. RAD51 loss of function abolishes gene targeting and de-represses illegitimate integration in the moss *Physcomitrella patens*. *DNA Repair* 9: 526–533.
- Schollmeyer JE. 1986. Identification of calpain II in porcine sperm. *Biology of Reproduction* 34: 721–731.
- Shaner NC, Campbell RE, Steinbach PA, Giepmans BNG, Palmer AE, Tsien RY. 2004. Improved monomeric red, orange and yellow fluorescent proteins derived from *Discosoma* sp. red fluorescent protein. *Nature Biotechnology* 22: 1567–1572.
- Tian Q, Olsen L, Sun B, Lid SE, Brown RC, Lemmon BE, Fosnes K, Gruis D (Fred), Opsahl-Sorteberg H-G, Otegui MS *et al.* 2007. Subcellular localization and functional domain studies of DEFECTIVE KERNEL1 in maize and *Arabidopsis* suggest a model for aleurone cell fate specification involving CRINKLY4 and SUPERNUMERARY ALEURONE LAYER1. *The Plant Cell* 19: 3127–3145.
- Tran D, Galletti R, Neumann ED, Dubois A, Sharif-Naeini R, Geitmann A, Frachisse JM, Hamant O, Ingram GC. 2017. A mechanosensitive Ca²⁺ channel activity is dependent on the developmental regulator DEK1. *Nature Communications* 8: 1009.
- Trouiller B, Schaefer DG, Charlot F, Nogué F. 2006. MSH2 is essential for the preservation of genome integrity and prevents homeologous recombination in the moss *Physcomitrella patens*. *Nucleic Acids Research* 34: 232–242.
- Vanlandewijck M, Dadras MS, Lomnytska M, Mahzabin T, Miller ML, Busch C, Brunak S, Heldin CH, Moustakas A. 2018. The protein kinase SIK downregulates the polarity protein Par3. *Oncotarget* 9: 5716–5735.
- Viaene T, Landberg K, Thelander M, Medvecka E, Pederson E, Feraru E, Cooper ED, Karimi M, Delwiche CF, Ljung K *et al.* 2014. Directional auxin transport mechanisms in early diverging land plants. *Current Biology* 24: 2786–2791.
- Wang C, Barry JK, Min Z, Tordsen G, Rao AG, Olsen OA. 2003. The Calpain Domain of the maize DEK1 protein contains the conserved catalytic triad and functions as a cysteine proteinase. *Journal of Biological Chemistry* 278: 34467–34474.
- Weill U, Krieger G, Avihou Z, Milo R, Schuldiner M, Davidi D. 2019. Assessment of GFP tag position on protein localization and growth fitness in yeast. *Journal of Molecular Biology* 431: 636–641.
- Whitewoods CD, Cammarata J, Nemeček V, Sang S, Crook AD, Aoyama T, Wang XY, Waller M, Kamisugi Y, Cumming AC *et al.* 2018. CLAVATA was a genetic novelty for the morphological innovation of 3D growth in land plants. *Current Biology* 28: 2365–2376.e5.
- Zhao S, Liang Z, Demko V, Wilson R, Johansen W, Olsen O-A, Shalchian-Tabrizi K. 2012. Massive expansion of the calpain gene family in unicellular eukaryotes. *BMC Evolutionary Biology* 12: 193.

Supporting Information

Additional Supporting Information may be found online in the Supporting Information section at the end of the article.

Fig. S1 Cre recombinase treatment evaluation.

Fig. S2 Southern blot analysis of dek1-pArrowf1-1 and dek1-tomato^{int} strains.

Fig. S3 Bud count analysis of dek1-tomato^{int} and dek1-tomato^{int}/dek1.

Fig. S4 Gametangia development is morphologically similar between WT and dek1-tomato^{int}.

Fig. S5 Spermatozooids are morphologically similar in WT and dek1-tomato^{int}.

Fig. S6 DEK1-TOMATO^{INT} during bud formation.

Fig. S7 DEK1-TOMATO^{INT} localizes at the plasma membrane.

Fig. S8 DEK1-TOMATO^{INT} is present in developing phyllids but absent in the mature phyllid.

Fig. S9 DEK1-TOMATO^{INT} during antheridia development.

Fig. S10 Schematic representation of the dek0 generation in the dek1-tomato^{int} background and transformant PCR genotyping.

Fig. S11 dek1-tomato^{int}/dek1^o transcript analysis.

Fig. S12 dek1-tomato^{int}/dek1^o transcript sequence analysis.

Table S1 List of the primers used in this study.

Please note: Wiley Blackwell are not responsible for the content or functionality of any Supporting Information supplied by the authors. Any queries (other than missing material) should be directed to the *New Phytologist* Central Office.